

**C₂D₅I DISSOCIATION AND D + CH₃ → CH₂D + H AT HIGH
TEMPERATURE: IMPLICATIONS TO THE HIGH PRESSURE
RATE CONSTANT FOR CH₄ DISSOCIATION**

by

M.-C. Su,[#] and J. V. Michael*

Chemistry Division, Argonne National Laboratory, Argonne, IL 60439, USA

Corresponding Author: **Dr. J. V. Michael**
D-193, Bldg. 200
Argonne National Laboratory
Argonne, IL 60439, USA
Phone: (630) 252-3171, Fax: (630) 252-4470
E-mail: Michael@anlchm.chm.anl.gov

(29th Symp. (Int'l) on Combust., revised, 4/16/02: Publication Number 1b03)

Presentation Mode: Oral Presentation
Preferred Publication: Proceedings
Category: Reaction Kinetics

	Text	Reference	Tables	Figures	Total
Count	6 pages	25 citations	3 pages	5 pages	
Equiv. Words	2594	502	1200	1000	5296

The submitted manuscript has been created by the University of Chicago as Operator of Argonne National Laboratory ("Argonne") under Contract No. W-31-109-ENG-38 with the U.S. Department of Energy. The U.S. Government retains for itself, and others acting on its behalf, a paid-up, nonexclusive, irrevocable worldwide license in said article to reproduce, prepare derivative works, distribute copies to the public, and perform publicly and display publicly, by or on behalf of the Government.

#Faculty Research Participant, Department of Educational Programs, Argonne, permanent address: Department of Chemistry, Butler University, Indianapolis, IN 46208.

This work was supported by the U. S. Department of Energy, Office of Basic Energy Sciences, Division of Chemical Sciences, under Contract No. W-31-109-Eng-38.

Abstract

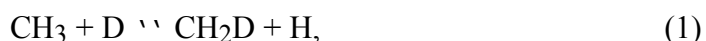
The shock tube technique with H- and D-atom atomic resonance absorption spectrometry (ARAS) detection has been used to study the thermal decomposition of C₂D₅I and the reaction,



over the temperature ranges, 924-1370 K and 1294–1753 K, respectively. First-order rate constants for the thermal decomposition of C₂D₅I can be expressed by the Arrhenius equation, $\log k_{\text{C}_2\text{D}_5\text{I}} = (10.397 \pm 0.297) - (7700 \pm 334 \text{ K})/T$, giving $k_{\text{C}_2\text{D}_5\text{I}} = 2.49 \times 10^{10} \exp(-17729 \text{ K}/T) \text{ s}^{-1}$. The branching ratio between product channels, C₂D₅ + I and C₂D₄ + DI, was also determined. These results coupled with the fast decomposition of C₂D₅ radicals were then used to specify [D]_i in subsequent kinetics experiments with CH₃ where [CH₃]₀ was prepared from the concurrent thermal decomposition of CH₃I. Within experimental error, the rate constants for reaction (1) were found to be temperature independent with $k_1 = (2.20 \pm 0.22) \times 10^{-10} \text{ cm}^3 \text{ molecule}^{-1} \text{ s}^{-1}$. The present data have been combined with earlier lower temperature determinations and the joint database has been examined with unimolecular rate theory. The implications of the present study can be generalized to supply a reliable value for the high-pressure limiting rate constant for methane dissociation.

Introduction

The $\text{CH}_3 + \text{H}$ reaction has been suggested to be of importance in such diverse systems as planetary atmospheres [1] and combustion [2]. Of particular importance is the limiting high-pressure rate constant. It has been recognized that information on the high-pressure limit can be obtained by studying the isotopic variation of the reaction,



and, to date, two studies at low temperatures have been published [3,4]. In the latter study at 300 K [4] the reaction was found to be ~92% of the high-pressure limit meaning that 8% of the initially formed vibrationally hot adduct molecules either reflect back to reactants or are stabilized by collisions. Stabilization was found to be almost negligible under the low-pressure conditions of the experiments. Hence, the measured value, $k_1(300 \text{ K}) = (2.13 \pm 0.13) \times 10^{-10}$, was corrected to give $k_{1\infty} = 2.3 \times 10^{-10}$ where both values are in $\text{cm}^3 \text{ molecule}^{-1} \text{ s}^{-1}$. Applying reduced mass corrections suggested a 300 K high-pressure value for $\text{H} + \text{CH}_3$ of $(2.9 \pm 0.7) \times 10^{-10} \text{ cm}^3 \text{ molecule}^{-1} \text{ s}^{-1}$. High-pressure limiting rate constants are necessary to theoretically rationalize the reverse process, $\text{CH}_4 \rightleftharpoons \text{CH}_3 + \text{H}$, at high temperatures [5], and, even though there are theoretical estimates, there are no measured high-T values for this rate constant. This has supplied the motivation for the present work on reaction (1).

Including the possibility of collisional deactivation for the present chemically activated case, the rate constant based on D-atom depletion at any pressure or temperature can be expressed in an RRK (or RRKM) formulation as:

$$k_D = k_{1\infty} \int_{\varepsilon_0}^{\infty} ((k_{f\varepsilon} + \beta\omega)/(k_{f\varepsilon} + k_{b\varepsilon} + \beta\omega)) f(\varepsilon) d\varepsilon \quad (2)$$

where $k_{1\infty}$, $k_{f\varepsilon}$, $k_{b\varepsilon}$, β , ω , and $f(\varepsilon)$ refer to (a) the high-pressure rate constant for reaction (1), (b) the specific RRK (or RRKM) rate constant for forward dissociation from CH_3D^* , (c) the specific RRK (or RRKM) rate constant for backward dissociation to give reactants at the threshold energy, ε_0 , (d) the collisional deactivation efficiency, (e) the collision rate constant, and (f) the normalized chemical activation distribution function originating at ε_0 for a given temperature, respectively. In the present case, the pressure is relatively low and the temperature is high suggesting that stabilization can never compete with both forward and back dissociations. Hence, the rate constant becomes, $k_D = k_{1\infty} \langle k_{f\varepsilon}/(k_{f\varepsilon} + k_{b\varepsilon}) \rangle$, where the average is taken over the distribution function, $f(\varepsilon)$, and this is then equal to the rate constant for reaction (1); that is, $k_D = k_1$.

In the present study, rate constants for reaction (1) were measured using the thermal dissociation of $\text{C}_2\text{D}_5\text{I}$ as the source of D-atoms. CH_3 -radicals were produced from the thermal dissociation of CH_3I [6]. Both D-depletion and H-formation experiments were performed, and the experiments were carried out with at least a six-fold excess of CH_3 so that the decay of D-atoms and the formation of H-atoms would be approximately pseudo-first-order.

Experimental

The present experiments were performed with the shock tube technique using atomic resonance absorption spectrometric (ARAS) detection. The method and the apparatus currently being used have been previously described [7,8]. Therefore, only a brief description of the experiment will be presented here.

The apparatus consists of a 7-m (4-in. o.d.) 304 stainless steel tube separated from the He driver chamber by a 4-mil unscored 1100-H18 aluminum diaphragm. The tube was routinely pumped between experiments to $<10^{-8}$ Torr by an Edwards Vacuum Products Model CR100P packaged pumping system. The velocity of the shock wave was measured with eight equally spaced pressure transducers (PCB Piezotronics, Inc., Model 113A21) mounted along the end portion of the shock tube, and temperature and density in the reflected shock wave regime were calculated from this velocity and include corrections for boundary layer perturbations [9-11]. The 4094C Nicolet digital oscilloscope was triggered by delayed pulses that derive from the last velocity gauge signal.

H- and D-atom atomic resonance absorption spectrometric (ARAS) detection was used to follow $[H]_t$ and $[D]_t$ quantitatively as described previously [12,13,14]. Adding small amounts of D_2 to the resonance lamp gave measurable Lyman- α D. Since the separation between H- and D-Lyman- α lines is substantial [14], the D-line was isolated by using an H-atom atomic filter (a slowly flowing H_2 discharge flow system) between the resonance lamp and the shock tube window in the kinetics experiments [15]. This was necessary because Lyman- α H is still present in the unfiltered lamp. The entire photometer system was radially located at the distance of 6 cm from the endplate. MgF_2

components were used in the photometer optics. The resonance lamp beam was detected by an EMR G14 solar blind photomultiplier tube, and typical experimental results are shown in Figs. 1 and 2.

Gases. High purity He (99.995%), used as the driver gas, was from AGA Gases. Scientific grade Kr (99.999%), the diluent gas in reactant mixtures, was from Spectra Gases, Inc. The ~10 ppm impurities (N₂ - 2 ppm, O₂ - 0.5 ppm, Ar - 2 ppm, CO₂ - 0.5 ppm, H₂ - 0.5 ppm, CH₄ - 0.5 ppm, H₂O - 0.5 ppm, Xe - 5 ppm, and CF₄ - 0.5 ppm) are all either inert or in sufficiently low concentration so as to not perturb H or D-atom profiles. Ultra-high purity grade He (99.999%) for the resonance lamp and high purity H₂ (99.995%) for the atomic filter were from AGA Gases. Research Grade D₂ (99.99%) from Air Products and Chemicals, Inc. was used in the resonance lamp. Analytical grade CH₃I (99%), C₂H₅I (99%), and C₂D₅I (99%), all from Aldrich Chemical Co. Inc., were purified by bulb-to-bulb distillation, retaining only the middle thirds. Test gas mixtures were accurately prepared from pressure measurements using a Baratron capacitance manometer and were stored in an all glass vacuum line.

Results and Discussion

Preliminary experiments on the thermal decomposition of C₂D₅I had to be carried out before studies on reaction (1) could proceed. Since we were primarily interested in the yield of D-atoms from the dissociation, the experiments were designed to measure D-atom formation and the approach to steady-state. These experiments closely followed the procedures given in our earlier decomposition study on C₂H₅I [13], and will not be repeated here. The results are tabulated in Table 1 and plotted in Fig. 3. The data can be represented in first-order by the equation, $\log(k_{C_2D_5I}/s^{-1}) = (10.397 \pm 0.297)$

– $(7700 \pm 334 \text{ K})/T$, giving $k_{\text{C}_2\text{D}_5\text{I}} = 2.49 \times 10^{10} \exp(-17729 \text{ K}/T) \text{ s}^{-1}$. The ratio of the protonated case [13] to this expression is $0.255 \exp(1835 \text{ K}/T)$, giving values ranging from 1.75 to 1.02 between 950 and 1320 K, respectively. Since both sets are only accurate to within $\sim\pm 40\%$, there is little difference in the overall rate constants for the two isotopic cases. In the earlier work [13], the branching ratio of $\text{C}_2\text{H}_5 + \text{I}$ to the total decomposition rate was found to be (0.87 ± 0.11) . Theoretical calculations could rationalize this result suggesting values varying with temperature from ~ 0.82 to 0.91 between 900 and 1300 K, respectively. For $\text{C}_2\text{D}_5\text{I}$, we have determined the branching ratio at various temperatures, and these are likewise given in Table 1. In this case, the values are somewhat less than in the protonated case suggesting relatively more importance for the elimination channel. The two decomposition processes can be accounted for in the modeling calculations for reaction (1) as shown in Table 2 where the rate constants for $\text{C}_2\text{D}_5\text{I}$ (k_{0a} and k_{0b}) are partitioned by the measured branching ratio.

Experiments were carried out by observing D-atom decay and H-atom build-up in separate experiments. Figures 1 and 2 shown typical examples of both types of experiments. Since the system is complex, modeling is required to determine k_1 . We used a twenty-three step mechanism from a previous study on the $\text{CH}_3 + \text{H}_2$ and the thermal decomposition of CH_4 [5] along with the additional reactions listed in Table 2. Hence the mechanism contained thirty-three reactions. We did not include $\text{CH}_3 + \text{H} + \text{Kr} \rightleftharpoons \text{CH}_4 + \text{Kr}$ and the deuterated analogs because our previous theoretical estimates of this rate constant [5] under the present conditions showed it to be entirely negligible. This conclusion was further confirmed by performing experiments using $\text{C}_2\text{H}_5\text{I}$ and CH_3I (i. e., H and CH_3). We found that H was not depleted, showing that no reaction occurred

between H and CH₃ on the time scale of the present study. This observation also completely rules out the abstraction processes, CH₃ + H ⇌ CH₂ + H₂ and deuterated analogs. In addition to reaction (1), the isotopic mixing reactions (2) to (6) in Table 2 were included in the mechanism. This was necessary because [D] reaches a steady-state as shown in Fig. 2. The experimental values of Seakins et al. [4] were used for reactions (3) and (5); however, for the back processes, (2), (4), and (6), equilibrium constants were calculated from the frequencies and structures given by Seakins et al. [4]. The T-dependence of these equilibrium constants could be expressed to within ±1% over the present T-range by polynomial fits, and these are given as denominators in Table 2 for reactions (2), (4), and (6).

The experiments were then modeled using the entire set of reactions, giving fits like those shown in Figs. 1 and 2 (solid lines). In the fitting procedure, [C₂D₅I]₀ was allowed to vary slightly, either up or down, from the value calculated from mole fraction for a given experiment; however, no adjustment was necessary for over half of the thirty-one experiments shown in Table 3. The maximum adjustment was 10% with ±4.7% being the standard deviation over the entire thirty-one fits. This result strongly corroborates the measured branching ratio for C₂D₅I dissociation (reactions (0a) and (0b) in Table 2). The only unknown rate constant is then k₁, and the values obtained from these fits are given in Table 3. Since the sensitivity for both H- and D-atom detection is so high in the present experiments thereby reducing the importance of secondary reactions including radical-radical reactions, the thirty-three step mechanism can be considerably simplified. We removed all reactions except the thermal decompositions of CH₃I [6] and C₂D₅I (reactions (0a) and (0b) in Table 2), and the bimolecular reactions D + CH₃ and its reverse (reactions (1) and (2) in Table 2). For the same choice of k₁, the

fits were insignificantly different from the entire mechanism as shown specifically in the two examples, Figs. 1 and 2, where the reduced mechanism results are plotted as dashed lines. The subsequent isotopic mixing reactions (3)-(6) were also unimportant because at long times $[H]$ goes to a maximum steady-state value which forces the reverse of reaction (1) (i. e., reaction (2) in Table 2) to be more competitive for CH_2D -radicals than the subsequent reaction with D, reaction (3) in Table 2.

Theory: Troe fits [16] for the $D + CH_3$ reaction under the present conditions were performed with the same energy transfer parameter used in earlier work [5]. According to theory, pressure stabilization is negligible being <4% at 1300 K and <0.6% at 1800 K. This agrees with the conclusions based on the above mentioned $H + CH_3$ experiments.

As mentioned in the introduction, the overall rate for reaction (1) is then, $k_1 = k_{1\infty} \langle k_{f\varepsilon} / (k_{f\varepsilon} + k_{b\varepsilon}) \rangle = k_{1\infty} F$. Using the frequencies and structures given in Seakins et al. [4] and Sutherland et al. [5], we have evaluated the chemical activation distribution function, $f(\varepsilon)$, and specific RRKM rate constants for both forward and backward dissociations. The forward dissociation is 1.54 kcal mole⁻¹ lower lying than the backward path. Hence, the forward path is preferred as shown by Seakins et al, who reported a value for F of 0.92 at 300 K. To within 0.04%, we obtain a value for the fraction of

$$F = 0.98545 - 2.4766E-4 T + 2.1753E-7 T^2 - 9.7309E-11 T^3 + 1.7148E-14 T^4$$

for the temperature range, 250 to 1800 K. Hence, $F(300 \text{ K})$ is 0.928 in good agreement with Seakins et al. Klippenstein, Goergievski, and Harding [17] have also carried out extensive theoretical calculations on reaction (1) and find that F varies from 0.92 to 0.79 over the same T-range. We obtain $F(1800 \text{ K}) = 0.857$. Hence, their fraction shows slightly more T dependence than the present evaluation.

If $k_{1\infty}$ is known then k_1 can be determined. As in earlier work [5,6], high-pressure values have been calculated between 250–1800 K for $D + CH_3$ assuming that the transition-state is a Lennard-Jones complex. This model then presupposes that there is no barrier to reaction (1). $k_{1\infty}$ can be calculated from,

$$k_{1\infty} = \left(\frac{g^\ddagger}{g_1 g_2} \right) \sigma_{12}^2 \Omega(2, 2)^* \left(\frac{8\pi kT}{\mu} \right)^{\frac{1}{2}} \exp\left(\frac{\epsilon_{12}}{kT} \right), \quad (3)$$

where $g^\ddagger = 1$, $g_1 = g_{CH_3} = 2$, and $g_2 = g_D = 2$. CH_3 polarizability is derived by methods described in Hirschfelder, Curtiss, and Bird [18]. Then the interaction parameters are calculated from CH_3 and D polarizabilities as described by Cambi et al. [19]. This method in effect replaces the simple combining rules [18] for determining σ_{12} and ϵ_{12} . $k_{1\infty}$ can then be expressed by $1.777 \times 10^{-11} T^{0.36} \exp(60.6 \text{ K}/T) \text{ cm}^3 \text{ molecule}^{-1} \text{ s}^{-1}$ to within $\pm 0.6\%$ over the T -range 250-2000 K. $k_1 = k_{1\infty} F$ can now be evaluated and the results are shown as the dashed lines in Figs. 4 and 5. This simple theoretical approach predicts values in good agreement with the present determinations but is lower than the 300 K values of Brouard et al. [3] and Seakins et al. [4] by 12 and 36%. Klippenstein, Georgievski, and Harding [17] have also evaluated k_1 from a much more fundamental point of view. The potential energy of interaction was determined using ab initio methods, and then variable reaction coordinate transition state theory (VRC-TST) with a trajectory correction was used to determine theoretical values for k_1 . These are shown as the solid lines in Figs. 4 and 5. This calculation is in excellent agreement with measurements, being slightly high at 1700-2000 K by only 13%. Hence, both methods agree remarkably well with the experimental data.

The implications to the high-pressure limit for $\text{H} + \text{CH}_3$ can be easily assessed as discussed by Seakins et al. [4]. With the Lennard-Jones model, the rate constants are related by the ratio of inverse square roots of reduced masses between $\text{H} + \text{CH}_3$ and $\text{D} + \text{CH}_3$. This factor is 1.372 implying that the high-pressure limit for $\text{H} + \text{CH}_3$ from the present calculation is $k_{(\text{CH}_3+\text{H})\infty} = 2.438 \times 10^{-11} \text{ T}^{0.36} \exp(60.6 \text{ K/T}) \text{ cm}^3 \text{ molecule}^{-1} \text{ s}^{-1}$ (250-2000 K). This is identical to the previous estimate from this laboratory for T greater than ~ 1000 K giving the high-pressure rate constant for methane dissociation, $k_{(\text{CH}_4)\infty} = 5.087 \times 10^{19} \text{ T}^{-0.860} \exp(-54916 \text{ K/T}) \text{ s}^{-1}$ for $1600 \leq T \leq 4500 \text{ K}$ [6]. As pointed out in this earlier work [6], the T-dependent estimate for $k_{(\text{CH}_3+\text{H})\infty}$ is within $\sim 10\%$ of that needed by Seakins et al. [4] to explain the low-pressure values of Brouard et al. [3] with a Master's equation approach. The present estimate also agrees with previous theoretical calculations including that of Seakins et al. [4]. Hase et al. [20] used three earlier estimates of the potential energy surface [21-23] and obtained values that are within $\pm 20\%$ of the present determinations at both 300 and 1000 K. With canonical flexible transition state theory, Robertson et al. [24] also obtain theoretical values that agree well with the present estimate. Lastly, the most recent values by Klippenstein, Georgievski, and Harding [17] are only 11-30% higher than the present estimate. In earlier work from this laboratory [25], a similar relationship has been noted between the Lennard-Jones method and flexible transition state theory for estimating high-pressure limits. However the important point is that all theoretical values regardless of the degree of sophistication give values for the high pressure limit that are easily within a factor of two with one another.

Acknowledgments: The authors thank Drs. S. J. Klippenstein, Y. Georgievski, and L. B. Harding for providing theoretical estimates prior to publication. This work was

supported by the U. S. Department of Energy, Office of Basic Energy Sciences, Division of Chemical Sciences under Contract No. W-31-109-Eng-38.

References

- [1] Parkinson, C. D., Griffioen, E., McConnell, J. C., Ben Jaffel, L., Vidal-Madjar, A., Clarke, J. T., and Gladstone, G. R., *Geophys. Res. Lett.* 26:3177 (1999).
- [2] Warnatz J., *Combustion Chemistry* (Ed. W. C. Gardiner, Jr.), Springer-Verlag, New York, 1984, p. 197.
- [3] Brouard, M., Macpherson, M. T., and Pilling, M. J., *J. Phys. Chem.* 93:4047 (1989).
- [4] Seakins, P. W., Robertson, S. H., Pilling, M. J., Wardlaw, D. M., Nesbitt, F. L., Thorne, R. P., Payne, W. A., and Stief, L. J., *J. Phys. Chem. A*, 101:9974 (1997).
- [5] Sutherland, J. W., Su, M.-C., and Michael, J. V., *Int. J. Chem. Kinet.* 33:669 (2001).
- [6] Kumaran, S. S., Su, M.-C., and Michael, J. V., *Int. J. Chem. Kinet.* 29:535 (1997).
- [7] Michael, J. V., *Prog. Energy Combust. Sci.* 18:327 (1992).
- [8] Michael, J. V., *Advances in Chemical Kinetics and Dynamics* (Ed. J. R. Barker), JAI, Greenwich, 1992, Vol. I, pp. 47-112, for original references.
- [9] Michael, J. V. and Sutherland, J. W., *Int. J. Chem. Kinet.* 18:409 (1986).
- [10] Michael, J. V., *J. Chem. Phys.* 90:189 (1989).
- [11] Michael, J. V. and Fisher J. R., *Seventeenth International Symposium on Shock Waves and Shock Tubes* (Ed. Y. W. Kim) AIP Conference Proceedings 208, American Institute of Physics, New York, 1990, pp. 210-215.
- [12] Lim, K. P. and Michael, J. V., *Proc. Comb. Inst.* 25:713 (1994), and references therein.
- [13] Kumaran, S. S., Su, M.-C., Lim, K. P., and Michael, J. V., *Proc. Comb. Inst.* 26:605 (1996).
- [14] Michael, J. V. and Lifshitz, Assa, *Handbook of Shock Waves*, Vol. 3 ; G. Ben-

-
- Dor, O. Igra, T. Elperin, and A. Lifshitz, Eds., Academic Press, New York, pp. 77-105.
- [15] Fisher, J. R. and Michael, J. V., *J. Phys. Chem.* 94:2465 (1990).
- [16] Troe, J., *J. Chem. Phys.* 66:4745 (1977); *ibid.* 66:4758 (1977); Troe, J., *J. Phys. Chem.* 83:114 (1979); Troe, J., *Ber. Bunsenges. Phys. Chem.* 87:161 (1983); Gilbert, R. G., Luther, K., and Troe, J., *Ber. Bunsenges. Phys. Chem.* 87:169 (1983).
- [17] Klippenstein, S. J., Georgievski, Y. and Harding, L. B. *Proc. Comb. Inst.* 29:xxx (2002), this symposium.
- [18] Hirschfelder, J. O., Curtiss, C. F., and Bird, R. B., *Molecular Theory of Gases and Liquids*, Wiley: New York, 1966.
- [19] Cambi, R., Cappelletti, D., Liuti, G., and Pirani, F., *J. Chem. Phys.* 95:1852 (1991).
- [20] Hase, W. L., Mondro, S. L., Duchovic, R. J., and Hirst, D. M., *J. Am. Chem. Soc.* 109:2917 (1987).
- [21] Hirst, D. M., *Chem. Phys. Lett.* 122:225 (1985).
- [22] Brown, F. B. and Truhlar, D. G., *Chem. Phys. Lett.* 113:441 (1985).
- [23] Schlegel, H. B., *J. Phys. Chem.* 84:4530 (1986).
- [24] Robertson, S. H., Wagner, A. F., and Wardlaw, D. M., *J. Chem. Phys.* 103:2917 (1995).
- [25] Kumaran, S. S., Su, M.-C., Lim, K. P., Michael, J. V., Wagner, A. F., and Harding, L. B., *J. Phys. Chem.* 100:7541 (1996).

Table 1. Rate and Yield Data for C₂D₅I Thermal Decomposition

P_1 / Torr	T_5 / K ^a	M_s ^b	ρ_5 / (10 ¹⁸ cm ⁻³) ^a	k_{1st} / s ⁻¹	Yield ^c
--------------	------------------------	--------------------	--	-----------------------------	--------------------

$$X_{C_2D_5I} = 1.9442 \times 10^{-6}$$

5.94	1184	2.135	0.949	7310	0.59
5.92	1078	2.026	0.884	972	
5.92	1069	2.020	0.884	918	
5.93	1063	2.014	0.882	704	
5.94	1318	2.270	1.024	29786	0.64
5.93	1252	2.206	0.989	20414	0.59
5.91	1356	2.306	1.037	46293	0.68
5.88	1292	2.250	1.007	20880	0.64
5.92	1133	2.091	0.928	2754	0.63
5.96	924	1.864	0.797	167	

5.87	1483	2.423	1.086		0.71
5.89	1618	2.541	1.142		0.73
5.92	1590	2.517	1.138		0.75
5.94	1425	2.374	1.079		0.72

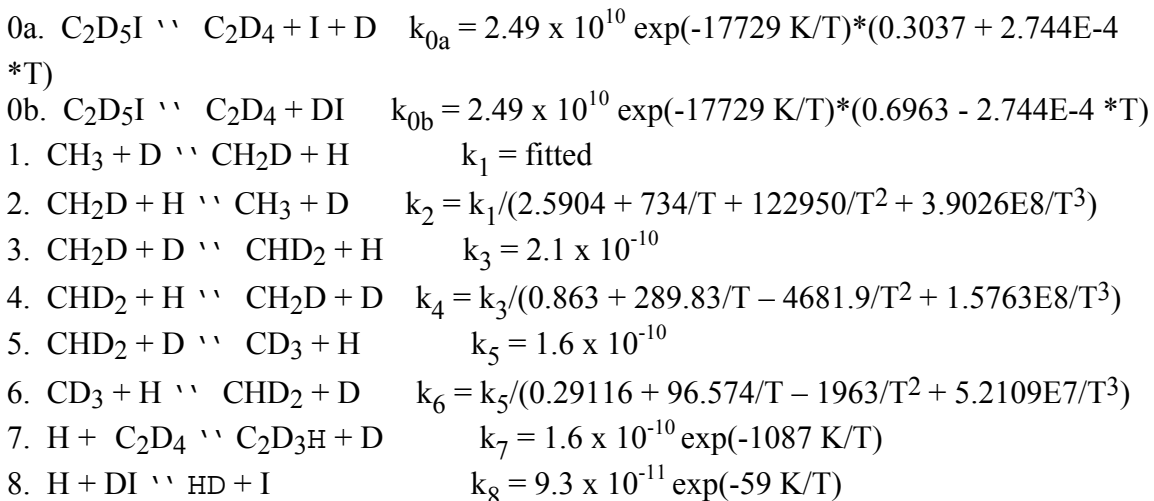
$$X_{C_2D_5I} = 5.9296 \times 10^{-7}$$

10.91	1370	2.324	1.937	73711	0.71
10.91	1272	2.234	1.860	29063	0.68
10.92	1129	2.091	1.717	5840	0.60
10.90	1012	1.966	1.579	481	
10.89	941	1.887	1.488	268	
10.87	1084	2.040	1.649	1900	0.62
10.95	1197	2.156	1.783	15454	0.64
10.98	1297	2.254	1.885	39082	0.68
10.95	1146	2.105	1.730	5450	0.68
10.92	1073	2.028	1.644	1958	
10.87	1011	1.961	1.564	683	
10.95	1017	1.968	1.583	644	

^aQuantities with the subscript 5 refer to the thermodynamic state of the gas in the reflected shock region. ^bThe error in measuring the Mach number, M_s , is typically 0.5-1.0 % at the one standard deviation level. ^cYield = $[D]_{\infty}/[C_2D_5I]_0$.

Table 2: Mechanism used for fitting [H] and [D] profiles.^a

The twenty-three reactions in Table 2 of ref. 5 were used in the fits along with the reactions listed below:



^aAll rate constants are in $\text{cm}^3 \text{ molecule}^{-1} \text{ s}^{-1}$.

Table 3: High Temperature Rate Data for D + CH₃

P_1 / Torr	T_5 / K ^a	M_s ^b	$\rho_5 / (10^{18} \text{ cm}^{-3})^a$	$k_1 / (10^{-10} \text{ cm}^3 \text{ s}^{-1})^c$
H-ARAS				
	$X_{\text{C}_2\text{D}_5\text{I}} = 7.907 \times 10^{-7}$		$X_{\text{CH}_3\text{I}} = 4.763 \times 10^{-6}$	
10.92	1505	2.446	2.047	2.40
10.95	1534	2.472	2.075	2.25
10.91	1672	2.591	2.163	2.20
10.91	1411	2.362	1.972	1.80
10.88	1661	2.577	2.139	2.30
	$X_{\text{C}_2\text{D}_5\text{I}} = 8.679 \times 10^{-7}$		$X_{\text{CH}_3\text{I}} = 5.403 \times 10^{-6}$	
10.89	1522	2.457	2.044	2.40
10.91	1649	2.567	2.137	2.00
10.96	1321	2.277	1.903	2.60
10.88	1419	2.365	1.962	1.90
10.95	1608	2.537	2.128	2.00
	$X_{\text{C}_2\text{D}_5\text{I}} = 7.254 \times 10^{-7}$		$X_{\text{CH}_3\text{I}} = 6.046 \times 10^{-6}$	
10.95	1586	2.518	2.113	2.30
10.94	1508	2.450	2.054	2.50
10.91	1462	2.408	2.012	2.20
10.94	1385	2.337	1.955	2.50
10.91	1696	2.611	2.178	2.50
10.97	1431	2.380	1.999	2.40

Table 3: High Temperature Rate Data for D + CH₃ (continued)

P_1 / Torr	T_5 / K ^a	M_s ^b	$\rho_5 / (10^{18} \text{ cm}^{-3})^a$	$k_1 / (10^{-10} \text{ cm}^3 \text{ s}^{-1})^c$
D-ARAS				
	$X_{\text{C}_2\text{D}_5\text{I}} = 8.679 \times 10^{-7}$		$X_{\text{CH}_3\text{I}} = 5.403 \times 10^{-6}$	
10.97	1502	2.440	2.044	1.95
10.97	1597	2.527	2.114	2.10
10.90	1294	2.248	1.858	2.50
10.96	1334	2.290	1.914	2.10
10.95	1543	2.476	2.071	1.90
	$X_{\text{C}_2\text{D}_5\text{I}} = 7.254 \times 10^{-7}$		$X_{\text{CH}_3\text{I}} = 6.046 \times 10^{-6}$	
10.95	1442	2.390	2.004	2.40
10.87	1622	2.549	2.122	2.30
10.88	1570	2.504	2.088	2.00
10.90	1411	2.362	1.970	2.15
10.95	1405	2.357	1.974	2.30
10.88	1565	2.499	2.084	2.10
10.98	1496	2.439	2.052	1.90
10.97	1333	2.289	1.915	2.10
10.90	1753	2.658	2.212	2.10
10.95	1599	2.529	2.121	2.10

^aQuantities with the subscript 5 refer to the thermodynamic state of the gas in the reflected shock region. ^bThe error in measuring the Mach number, M_s , is typically 0.5-1.0 % at the one standard deviation level. ^cRate constants for reaction (1) from simulations as described in the text.

Figure Captions

Fig. 1 H-atom profile ($[H]_t$ against time) for an experiment with $P_1 = 10.97$ Torr and $M_s = 2.380$. $T_5 = 1431$ K, $\rho_5 = 1.999 \times 10^{18}$ molecules cm^{-3} , $[CH_3I]_0 = 1.209 \times 10^{13}$ molecules cm^{-3} , and $[C_2D_5I]_0 = 1.450 \times 10^{12}$ molecules cm^{-3} . The mechanism shown in Table 1 was used to fit the profile giving the solid line. The dashed line is obtained with a highly reduced mechanism (see text). The second-order value for k_1 is 2.4×10^{-10} $\text{cm}^3 \text{molecule}^{-1} \text{s}^{-1}$ for this experiment.

Fig. 2 D-atom profile ($[D]_t$ against time) for an experiment with $P_1 = 10.95$ Torr and $M_s = 2.356$. $T_5 = 1405$ K, $\rho_5 = 1.974 \times 10^{18}$ molecules cm^{-3} , $[CH_3I]_0 = 1.194 \times 10^{13}$ molecules cm^{-3} , and $[C_2D_5I]_0 = 1.432 \times 10^{12}$ molecules cm^{-3} . The mechanism shown in Table 1 was used to fit the profile giving the solid line. The dashed line is obtained with a highly reduced mechanism (see text). The second-order value for k_1 is 2.3×10^{-10} $\text{cm}^3 \text{molecule}^{-1} \text{s}^{-1}$ for this experiment.

Fig. 3 Arrhenius plot from the data in Table 1 for the thermal decomposition of C_2D_5I .

Fig. 4 Arrhenius plot of the data from Table 3, (E) – H-atom experiments, (J) – D-atom experiments. The solid line is a theoretical calculation from ref. 17, and the dashed line is a theoretical calculation from this work.

Fig. 5 Arrhenius plot of the data from Table 3, (E) – H-atom experiments, (J) – D-atom experiments, along with those (B) from refs. 3 and 4. The solid line is a theoretical calculation from ref. 17, and the dashed line is a theoretical calculation from this work.

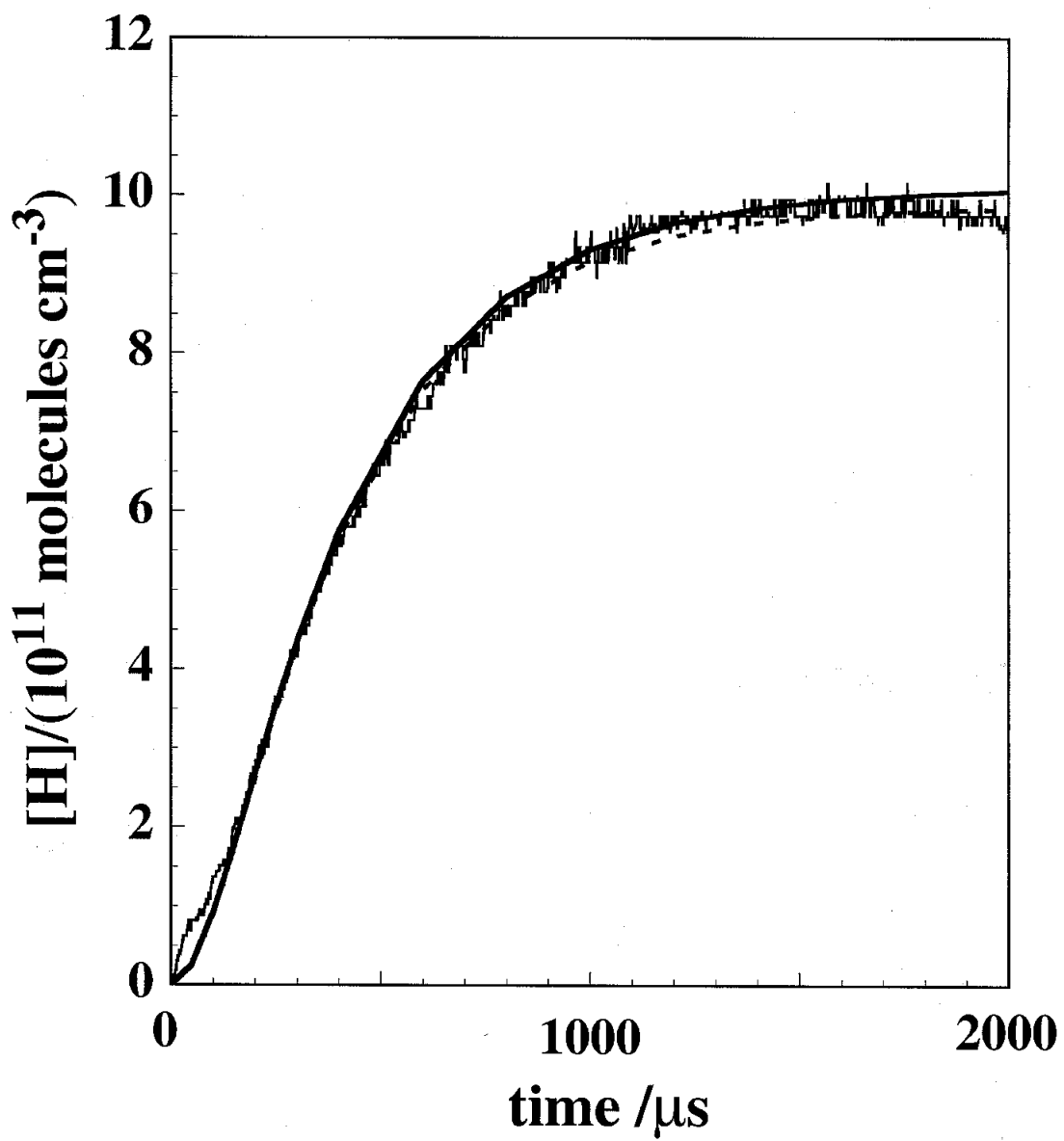


Figure 1

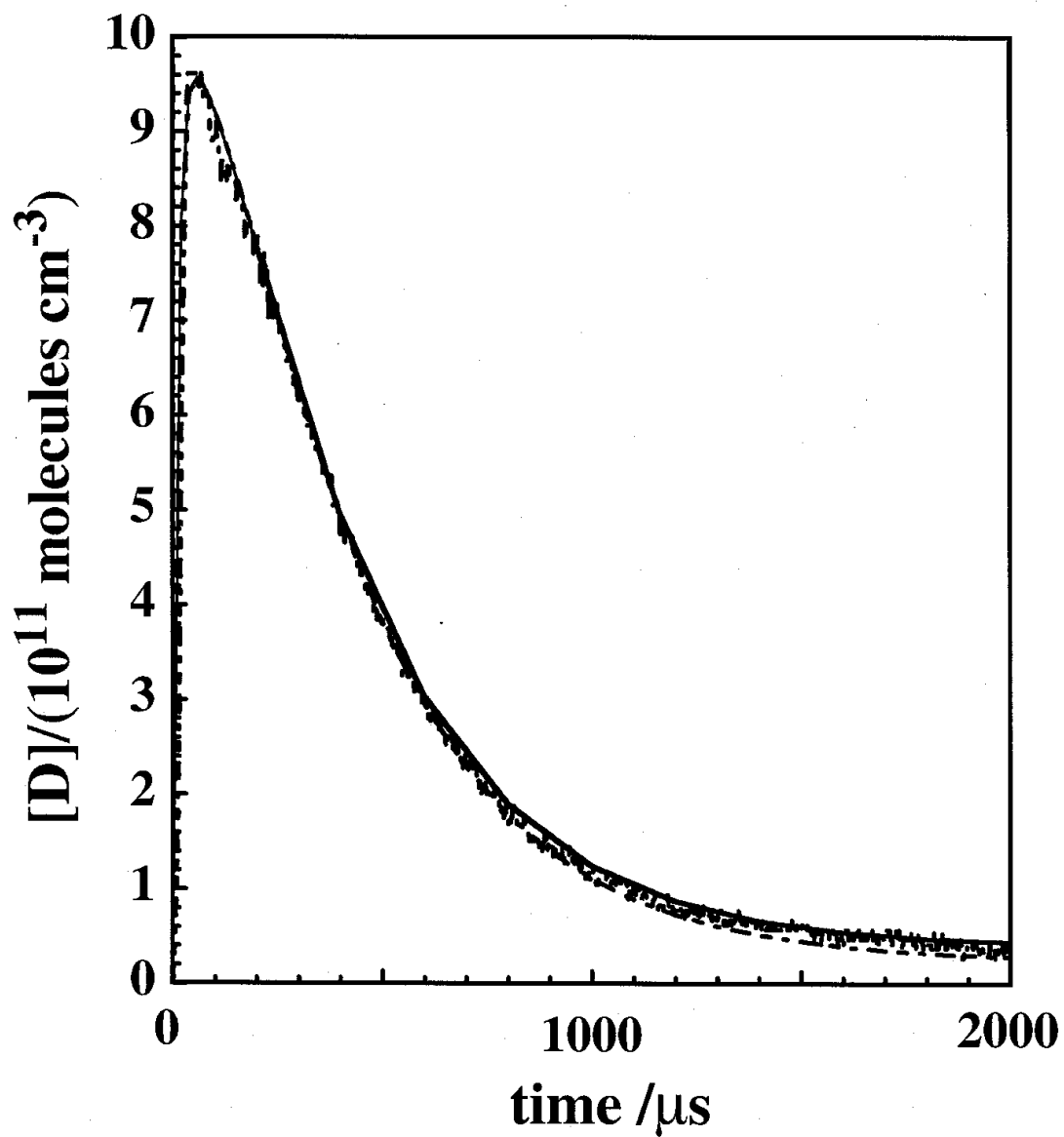


Figure 2

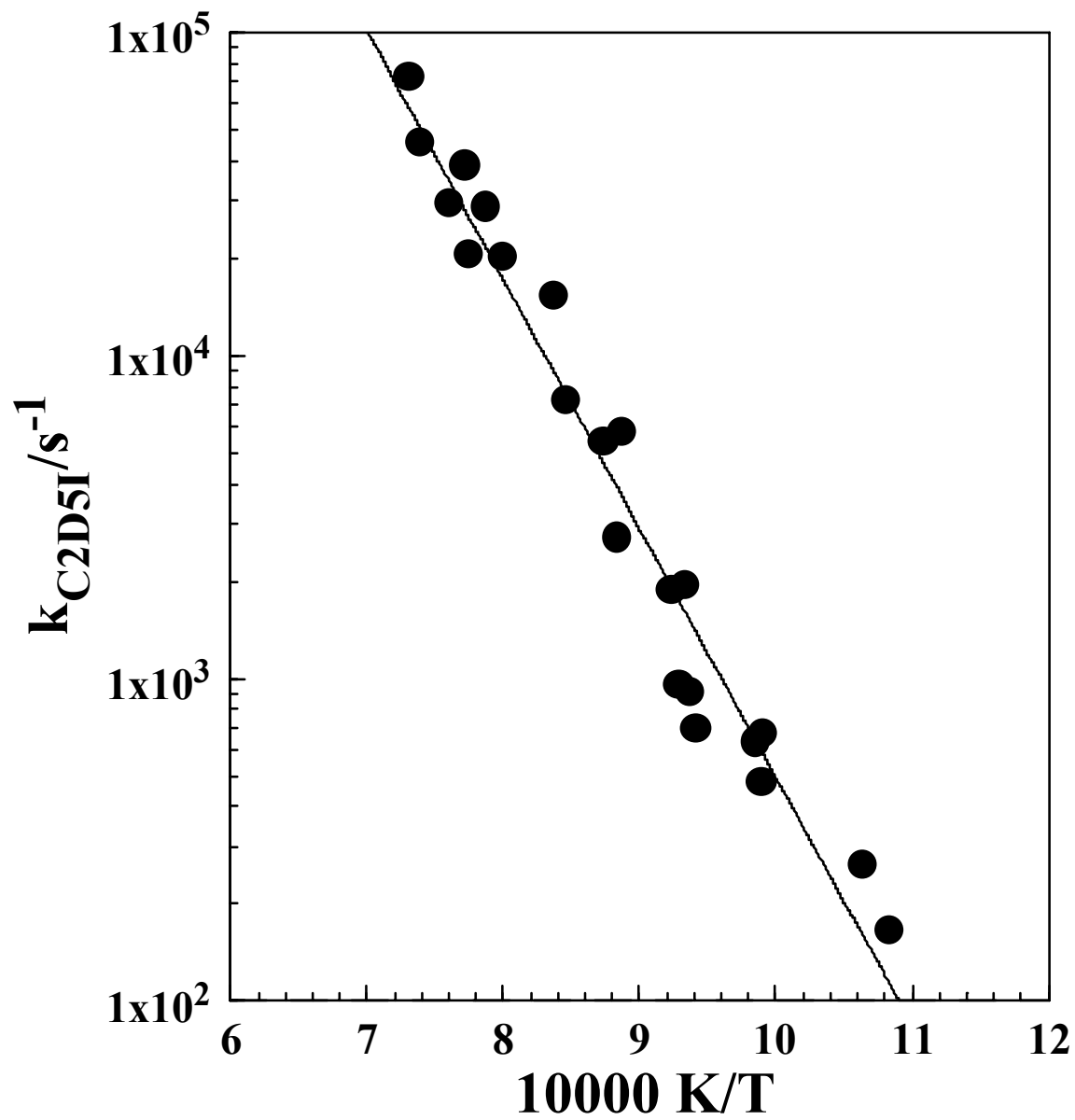


Figure 3

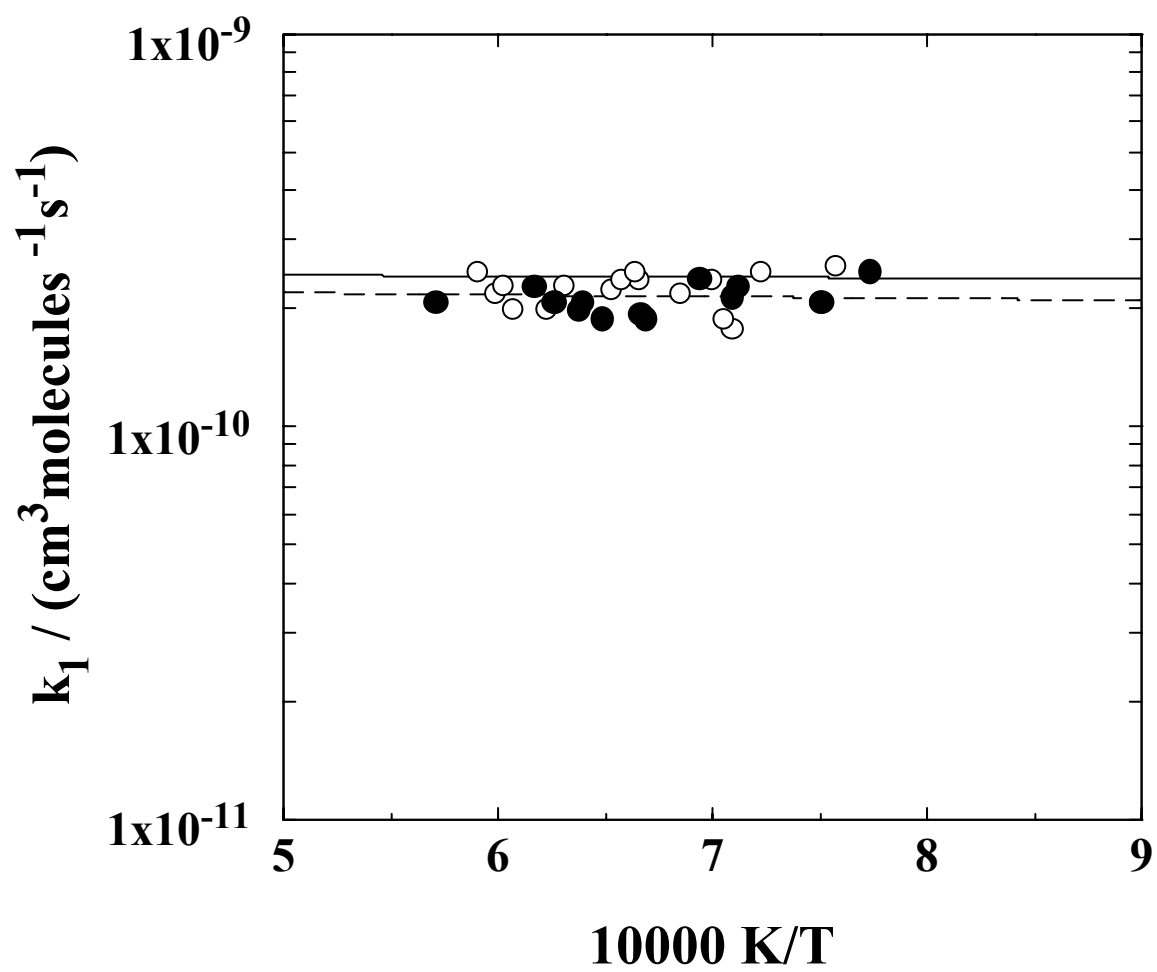


Figure 4

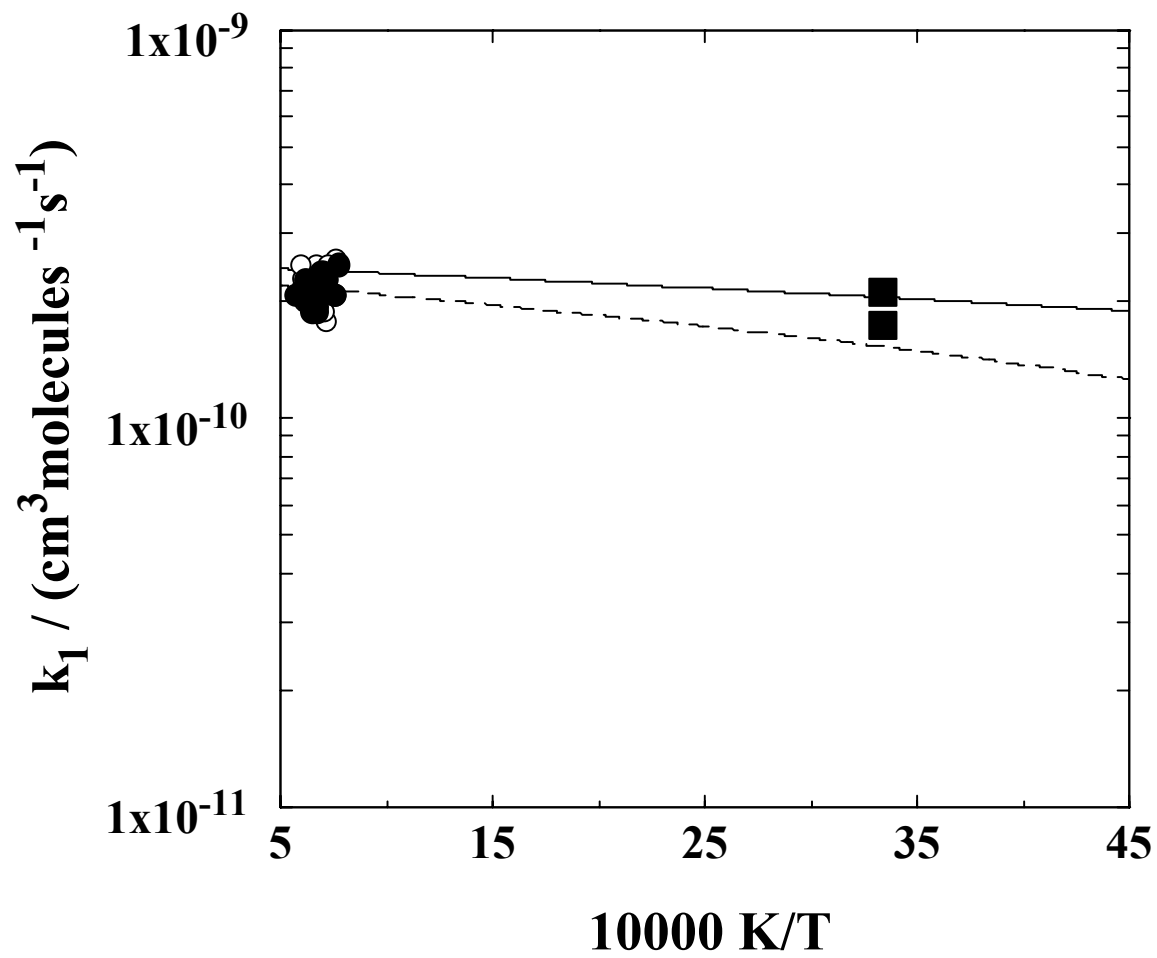


Figure 5